Available online at www.sciencedirect.com
ScienceDirect
Catalysis Today 117 (2006) 75–79
CATALYSIS TODAY
www.elsevier.com/locate/cattod

Activity pattern of low-loaded FeO_x/SiO_2 catalysts in the selective oxidation of C_1 and C_3 alkanes with oxygen

F. Arena [a,*], G. Gatti [b], L. Stievano [c], G. Martra [b], S. Coluccia [b], F. Frusteri [d], L. Spadaro [d], A. Parmaliana [a]

[a] *Dipartimento di Chimica Industriale e Ingegneria dei Materiali, Università degli Studi di Messina, Salita Sperone 31, 98166 S. Agata (Messina), Italy*
[b] *Dipartimento di Chimica IFM and NIS Center of Excellence, Università degli Studi di Torino, Via P. Giuria 7, 10125 Torino, Italy*
[c] *Laboratoire de Réactivité de Surface, Université Paris VI, UMR 7609, Place Jussieu 4, 75252 Paris, France*
[d] *Istituto CNR-ITAE "Nicola Giordano", Salita S. Lucia 39, I-98126 S. Lucia (Messina), Italy*

Available online 27 June 2006

Abstract

The structure and redox properties of *low-loaded* (0.015–0.73 wt% Fe) FeO_x/SiO_2 catalysts obtained by *adsorption–precipitation* of Fe^{2+} were probed by Mössbasuer and TPR techniques. Oxide dispersion data, obtained by deconvolution of Mössbasuer and TPR spectra, signal the *speciation* of the active phase into "*isolated*" *FeO_x sites*, "2-*d FeO_x patches*" and "3-*d Fe_2O_3 clusters*". The reactivity of FeO_x/SiO_2 catalysts in the selective oxidation of CH_4 and C_3H_8 in the range 475–650 °C has been assessed. Basic relationships amongst dispersion, specific rate of alkane conversion and product formation signal that the selective oxidation functionality depends upon local environment and oxygen bond strength of active sites, their distribution being closely related to the efficiency of synthesis route.

Keywords: FeO_x/SiO_2 catalysts; Light paraffins; Preparation method; Selective oxidation; Dispersion

1. Introduction

The direct conversion of natural gas (NG) streams into commodity chemicals constitutes nowadays one of the hottest topics in catalysis [1–3]. Potential alkanes activation routes based on novel catalytic approaches along with low-cost NG feedstock would in fact result in significant advantages over current technologies in terms of reduced dependence from oil, improved process economics and better environmental compatibility [1].

Various catalyst formulations for the selective oxy-functionalization of C1–C5 alkanes have been so far proposed [1–10], however the low productivity remains still the major drawback for industrial exploitation [1,2]. Although the oxy-functionalization of C1–C5 alkanes entails operating conditions and catalyst features specifically "tuned" on the reactivity of the substrate and required product(s) [7–10], these catalysts share some basic requirements mostly consisting in a high dispersion of active phases (*site isolation*) and "smoothed" acid–base characteristics in order to minimize product *adsorption* and *over-oxidation* phenomena [1–4].

A superior performance of FeO_x/SiO_2 catalysts in the selective oxidation of CH_4 to HCHO (MPO) has been recently recognised [2–4] yet, dispersion and local environment of Fe^{3+} centres decisively affect the overall activity–selectivity pattern [2–7].

Therefore, this paper shows the effects of the preparation method and loading on *speciation*, dispersion and reducibility of the active phase in *low-loaded* FeO_x/SiO_2 catalysts, addressing direct relationships amongst dispersion, activity and apparent activation energy which prove the key-role of dispersion on the oxidation path of both CH_4 and C_3H_8 substrates.

2. Experimental

2.1. Catalyst preparation

Commercial F5 and Si 4-5P silica samples (*AKZO NOBEL*) were used for preparation of FeO_x/SiO_2 catalysts either by *adsorption–precipitation* (AP) or *incipient wetness* (IW) routes [2–7], respectively. The list of the studied samples is given in Table 1.

* Corresponding author. Tel.: +39 090 676 5606; fax: +39 090 391 518.
E-mail address: Francesco.Arena@unime.it (F. Arena).

0920-5861/$ – see front matter © 2006 Elsevier B.V. All rights reserved.
doi:10.1016/j.cattod.2006.05.047

Table 1
List of the studied catalysts

Catalyst	Support	Preparation method	Fe loading (wt ppm)	SA_{BET} ($m^2\ g^{-1}$)	SSL ($Fe_{at}\ nm^{-2}$) × 10^2
S1	F5	–	150	607	0.3
S2	Si 4-5P	–	200	385	0.6
F[1000]S2-IW	Si 4-5P	IW–Fe^{III}	1000	402	2.7
F[4300]S2-IW	Si 4-5P	IW–Fe^{III}	4300	388	11.9
F[3700]S2-AP	Si 4-5P	AP–Fe^{II}	3700	399	10.0
F[1000]S1-AP	F5	AP–Fe^{II}	1000	601	1.8
F[3700]S1-AP	F5	AP–Fe^{II}	3700	597	6.7
F[5900]S1-AP	F5	AP–Fe^{II}	5900	592	10.8
F[7300]S1-AP	F5	AP–Fe^{II}	7300	581	13.5

2.2. Physico-chemical characterization

Physico-chemical characterization of the catalysts was performed by Mössbauer and TPR analyses [7]. Fitting of Mössbauer and TPR spectra was performed as elsewhere described [7] to get quantitative information on the structures of the various catalysts.

2.3. Catalyst testing

Catalyst testing in the selective oxidation of CH_4 (650 °C) and C_3H_8 (475–525 °C) has been performed by *differential* ''batch'' and ''continuous-flow'' reaction tests, feeding alkane–oxygen (C_nH_{2n+2}:O_2 = 2) mixtures at the rate of 1000 and 50 stp $cm^3\ min^{-1}$, respectively.

3. Results and discussion

3.1. Surface species, redox pattern and catalytic pattern

Mössbauer spectra at liquid He temperature (−269 °C) of representative catalysts outgassed at r.t. are shown in Fig. 1. At this temperature, Mössbauer spectroscopy allows to resolve the signal relative to aggregated superparamagnetic species exhibiting magnetically split spectral components from that of isolated paramagnetic iron species featuring quadrupole

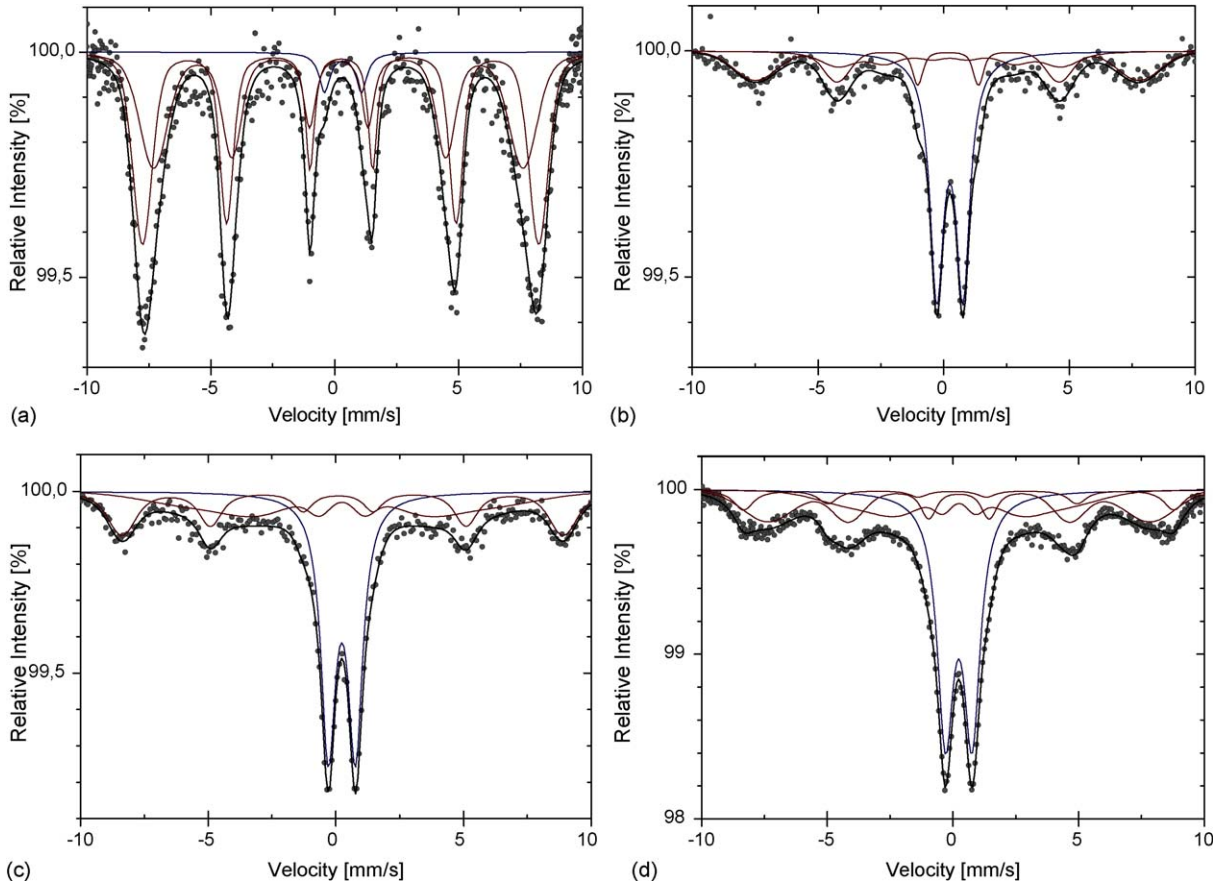

Fig. 1. Mössbauer spectra at −269 °C of F[4300]S2-IW (a), F[3700]S2-AP (b), F[3700]S1-AP (c) and F[7300]S1-AP (d) catalysts.

Table 2
Mössbauer spectral hyperfine parameters at −269 °C of the FeO_x/SiO_2 catalysts

Sample	B_{hf} (T)	QS (mm/s)	δ (mm/s)	LW (mm/s)	Area (%)	Surface species
F[4300]S2-IW	48.1(1)	0.02(1)	0.34(1)	–	95(1)	Oxide species
	–	1.15(7)	0.35(4)	0.5(1)	5(1)	Paramagnetic Fe(III)
F[3700]S2-AP	47.3(3)	−0.03(5)	0.27(3)	–	30(2)	Oxide species
	27.6(8)	0.0(2)	0.35(8)	–	16(2)	Oxide species
	–	1.04(1)	0.36(1)	0.66(2)	54(2)	Paramagnetic Fe(III)
F[3700]S1-AP	53.6(2)	0.17(4)	0.29(2)	–	27(3)	Oxide species
	34(2)	0.0(2)	0.35(7)	–	27(3)	Oxide species
	–	1.06(1)	0.35(4)	0.70(2)	46(2)	Paramagnetic Fe(III)
F[7300]S1-AP	53.1(2)	0.25(6)	0.25(4)	–	9(3)	Oxide species
	47.2(7)	0.0(2)	0.35(8)	–	26(4)	Oxide species
	24.7(8)	0.0(2)	0.35(8)	–	18(4)	Oxide species
	–	1.06(1)	0.34(1)	0.79(2)	45(1)	Paramagnetic Fe(III)

doublets. The values of hyperfine magnetic field "B_{hf}", quadrupole splitting "QS", isomer shift "δ" (relative to α-Fe), Lorentzian linewidth "LW" and relative resonance area of the spectral components resulting from the fitting of the experimental spectra are listed in Table 2.

The dominant six-line pattern in the spectrum of F[4300]S2-IW sample (Fig. 1a) indicates an overwhelming presence of superparamagnetic Fe_2O_3 particles with a mean size smaller than 8 nm [7,11]. The slight difference in the hyperfine parameters from those of α-Fe_2O_3 could be due to either the nanometric size or the low crystallinity of such particles [7,11].

Whereas, a dominant quadrupole doublet signals that on the counterpart F[3700]S2-AP (Fig. 1b), F[3700]S1-AP (Fig. 1c), F[7300]S1-AP (Fig. 1d) systems a relevant fraction of Fe^{3+} is present as *isolated ions* (Table 2). A δ range of 0.27–0.36 mm/s coupled to QS values of 1.02–1.15 mm/s matches the presence of Fe^{3+} ions in a somewhat distorted *high-spin* (O_h-like) coordination environment [7,11]. Moreover, a rather large value of the LW parameter (Table 2) suggests a rather inhomogeneous local symmetry of Fe ions belonging to isolated species and/or poorly crystallised very small iron oxide/hydroxides clusters.

The TPR profiles of various catalysts prepared by AP and IW routes using both S1 and S2 carriers are shown in Fig. 2. All the integral consumption data (up to 800 °C) correspond to a H_2/Fe ratio comprised between 0.42 and 0.56 (i.e., $Fe^{3+} \rightarrow Fe^{2+}$), diagnostic of a strongly inhibiting role of the silica matrix on the reduction of Fe ions to the metallic state [7].

A systematic shift of the reduction profile to lower temperature with rising the loading (Fig. 2A), more evident for IW and low surface area S2 catalysts, proves as a rule an easier

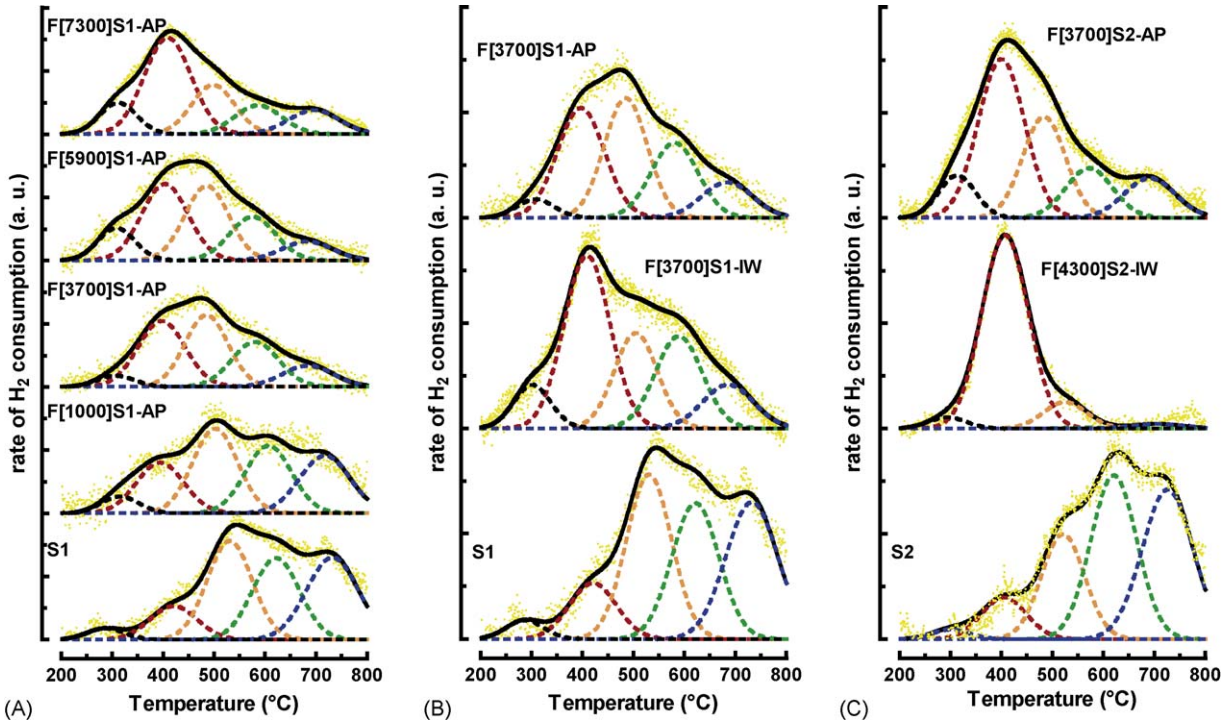

Fig. 2. TPR profiles of (A) F[xxxx]S1-AP catalysts; (B) S1 silica (a); F[3700]S1-IW (b) and F[3700]S1-AP (c) and (C) S2 silica (a); F[4300]S2-IW (b) and F[3700]S2-AP catalysts.

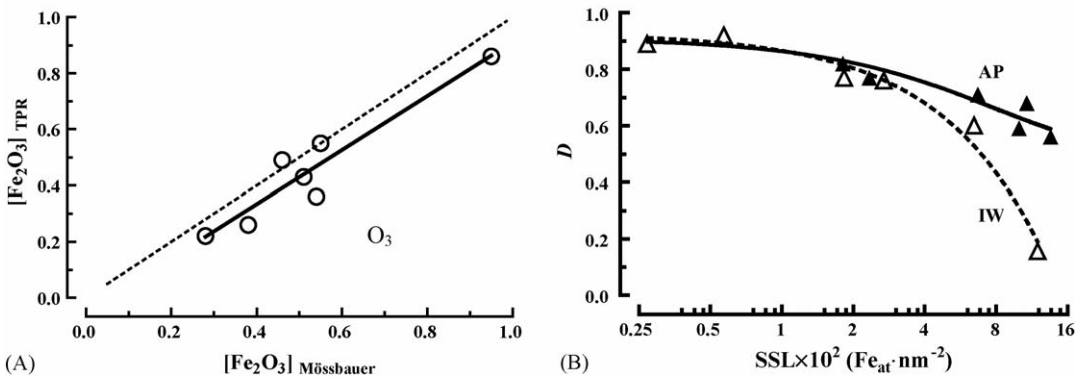

Fig. 3. (A) Relationship between concentration of Fe_2O_3 particles from modelling of TPR and Mössbauer spectra. (B) Dispersion of AP and IW catalysts vs. surface Fe loading (SSL).

reducibility induced by a lower dispersion of the active phase [7]. Despite the different qualitative features, all such spectra can be reproduced by a linear combination of five Gaussian peaks (Fig. 2) with analogous position and full-width-at-half-maximum [6,7]. Considering that a same chemical species must exhibit a same reactivity regardless of loading, preparation route and silica carrier, each Gaussian component can be associated to Fe^{3+} ions belonging to a same surface structure [6,7]. Namely, according to the above experimental evidences the first and second components, centred at ca. 300 and 400 °C, are associated with the reduction of Fe ions at the surface and in the bulk of 3-d Fe_2O_3 particles, respectively. The third component centred at ca. 500 °C arises from the reduction of 2-*d patches* (i.e., thin ''rafts''), while the 4th and 5th peaks, with maximum at ca. 600 and 700 °C, account for the poor reducibility of ''isolated'' Fe ions in a *low* and *high* degree of coordination with surface oxygen ions [6,7]. As observable from Fig. 3A, the substantial agreement between Mössbauer and TPR data on the relative amount of Fe_2O_3 particles supports the reliability of TPR analysis in getting insights into the surface structures of FeO_x/SiO_2 catalysts. Then the trends of dispersion, as calculated from the cumulative area of the 1st, 3rd, 4th and 5th Gaussian components [7], for both IW and AP catalysts are compared in Fig. 3B. The AP route ensures a much more effective Fe dispersion (0.90–0.60) regularly decreasing with the loading, while for the IW samples an extensive aggregation of Fe ions is particularly evident at SSL higher than 0.04 $Fe_{at}\ nm^{-2}$ [6,7].

Matching the above characterization findings, the catalytic data in the MPO reaction (650 °C) signals marked effects of the synthesis route and Fe loading on both activity and selectivity [7]. Although the Fe addition promotes the reactivity of any silica support, the AP route enables a systematically superior MPO performance owing to an improved dispersion of the active phase (Fig. 3B). This is evident from Fig. 4 showing the specific rate of CH_4 conversion (Fe_{CH_4}) and HCHO formation (Fe_{HCHO}, $Fe_{CH_4} \times S_{HCHO}$) of the iron atoms as a function of the FeO_x dispersion. The steady rise in activity ensured by an increasing availability of active sites is accompanied by a steeper increase of the HCHO production rate due to the positive effect of dispersion on HCHO selectivity. Then, adequate local ''environment'' of active sites, intermediate strength of the oxygen bonding in 2-*d patches* and low-coordinated *isolated* FeO_x species [7] along with a low ''availability'' of *nucleophylic* lattice oxygen species [2–4] well account for the positive effect of dispersion on the selective oxidation functionality of the FeO_x/SiO_2 system.

The activity pattern of FeO_x/SiO_2 catalysts in the POD reaction (475–525 °C) is outlined in Fig. 5 in terms of influence of dispersion on the Fe specific rate of C_3H_8 conversion (A), apparent activation energy (B) and product selectivity (C).

The FeO_x/SiO_2 catalysts denote a rather good performance also in the oxy-functionalization of propane yielding propylene and acrolein as main reaction products along with relatively low amounts (≈30%) of CO_x at any temperature. Structure, dispersion and reducibility of the active phase are yet crucial also for the POD pattern. In particular, the rising trends of $Fe_{C_3H_8}$ (Fig. 5A) signal that also in this case the dispersion is a key-parameter which overwhelms any effect of reducibility of the various species. The sharp rise of $Fe_{C_3H_8}$ with D, more evident at higher temperature, mirrors in fact the catalytic pattern of more dispersed FeO_x species with a stronger oxygen bonding [7], leading to a parallel increase of E_{app} (Fig. 5B). Therefore, matching with the occurrence of a consecutive $C_3H_8 \rightarrow C_3H_6 \rightarrow C_3H_4O \rightarrow CO_x$ reaction path [9], the rise in C_3H_6 selectivity (Fig. 5C) proves the rising contribution of ''isolated'' species against that of oxide particles leading to the propylene (*over*)oxidation on poorly dispersed systems.

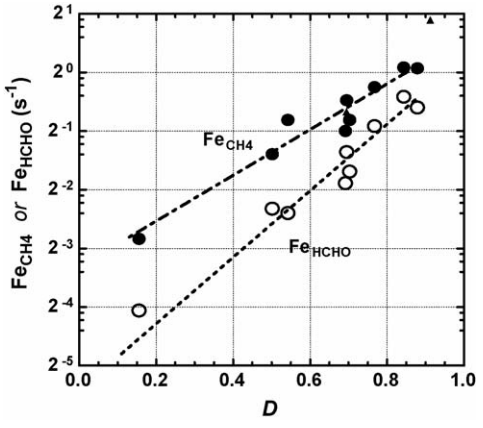

Fig. 4. Effect of dispersion (D) on the specific rates (s^{-1}) of CH_4 conversion (Fe_{CH_4}) and HCHO formation (Fe_{HCHO}) of FeO_x/SiO_2 catalysts (*T*, 650 °C).

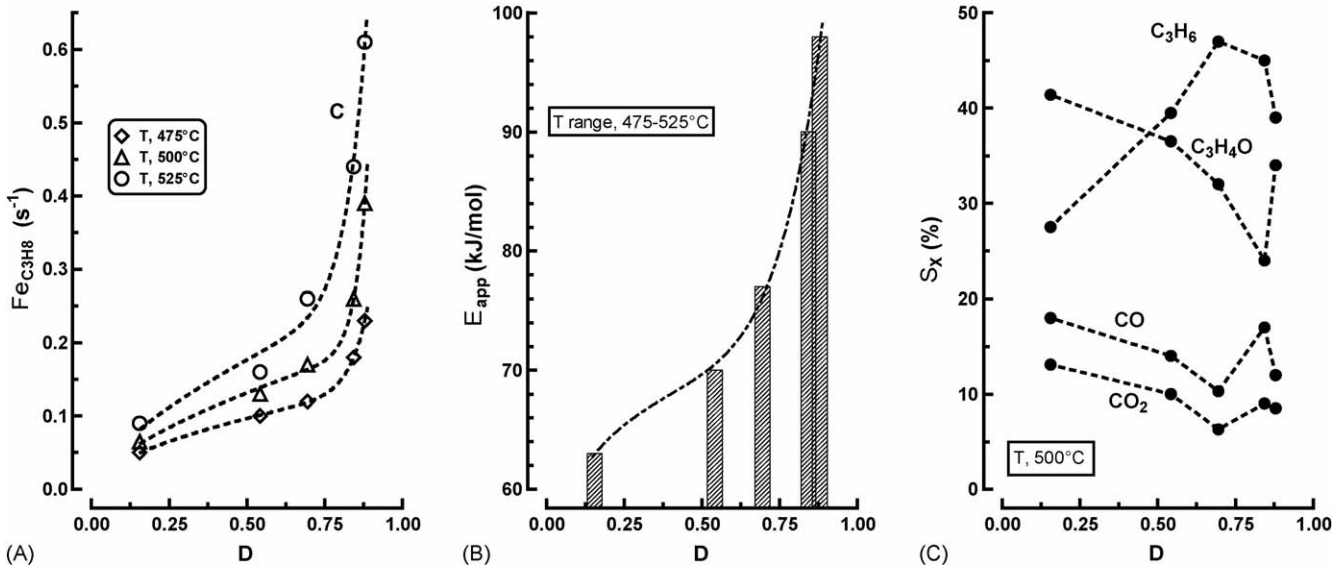

Fig. 5. Effect of dispersion (D) on the Fe atom specific rate ($Fe_{C_3H_8}$) of C_3H_8 conversion (A), apparent activation energy (B) and product selectivity at 500 °C (C) in the POD reaction.

References

[1] S. Albonetti, F. Cavani, F. Trifirò, Catal. Rev. Sci. Eng. 38 (4) (1996) 413.
[2] F. Arena, A. Parmaliana, Acc. Chem. Res. 36 (12) (2003) 687.
[3] T. Kobayashi, Catal. Today 71 (2001) 69.
[4] F. Arena, A. Parmaliana, Rec. Res. Dev. Catal. 2 (2003) 251.
[5] A. Parmaliana, F. Arena, F. Frusteri, A. Mezzapica, German Patent GEM 17 (2000) by SÜD CHEMIE AG. (Munich, Germany).
[6] F. Arena, G. Gatti, G. Martra, S. Coluccia, A. Parmaliana, Catal. Today 91–92 (2004) 305.
[7] F. Arena, G. Gatti, G. Martra, S. Coluccia, L. Stievano, L. Spadaro, P. Famulari, A. Parmaliana, J. Catal. 231 (2005) 365.
[8] E. Balcells, F. Borgmeier, I. Griβtede, H.-G. Lints, F. Rosokowski, Appl. Catal. A 266 (2004) 211.
[9] J.M. Oliver, J.M. López Nieto, P. Botella, Catal. Today 96 (2004) 241.
[10] E. Heracleous, M. Machli, A.A. Lemonidou, I.A. Vasalos, J. Mol. Catal. A 232 (2005) 29.
[11] A.W. Holland, G. Li, A.M. Shahin, G.J. Long, A.T. Bell, T.D. Dilley, J. Catal. 235 (2005) 150.